Guesdon *et al. Stem Cell Research & Therapy* (2025) 16:427
https://doi.org/10.1186/s13287-025-04552-7

Stem Cell Research & Therapy

SHORT REPORT

Repair of infarcted myocardium by skeletal muscle-derived mesenchymal stromal cells delivered by a bioprinted collagen patch

Rose Guesdon[1,2*], Serena Santoro[1], Audrey Cras[3], Etienne Pagin[2], Didier Serteyn[4], Justine Ceusters[4], Fabien Guillemot[2], Albert Hagège[5] and Philippe Menasché[1,6*]

Abstract

Mesenchymal stromal cells (MSC) are commonly investigated for post-infarction cardiac repair because of their angiogenic, anti-inflammatory and immunomodulatory properties. However, autologous sources (bone marrow and adipose tissue) require substantially invasive harvest procedures while allogeneic MSC from the cord raise the issue of batch to batch variability. This study assessed the effects of another under-investigated cell source: the skeletal muscle whose autologous MSC feature the clinically appealing advantage of being retrievable by a minimally invasive microbiopsy. MSC differentiated from induced pluripotent stem cells (iPSC) were selected as controls as they also look clinically attractive because of their high scalability and high degree of reproducibility. In vitro, muscle-derived (md) MSC exhibited typical MSC features including a tri-lineage differentiation potential and had robust angiogenic, anti-inflammatory, anti-fibrotic and immune-modulatory effects. Overall, they outperformed iPSC-MSC which raised a safety concern linked to the persistence of some pluripotency-associated markers. They were thus chosen for the subsequent in vivo evaluation in a rat model of left ventricular (LV) dysfunction induced by ischemia/reperfusion. To this end, mdMSC were embedded in a collagen bioprinted gel; the resulting epicardially-delivered patch significantly improved LV ejection fraction compared to a cell-free patch and sham-operated controls. Transcriptomic analysis revealed that this benefit was accompanied by a downregulation of fibrosis-, apoptosis-, and inflammation-related genes. This exploratory proof-of-concept study thus suggests that mdMSC offer an attractive alternative because they combine an autologous origin with a minimally invasive harvest procedure. Bioprinting these cells with a collagen bioink allows to generate a patch endowed with cardio-reparative properties.

Keywords Heart failure, Stem cell therapy, Mesenchymal stromal cells, Cardiac patch

*Correspondence:
Rose Guesdon
rose.guesdon@inserm.fr
Philippe Menasché
philippe.menasche@aphp.fr
[1] Inserm UMR 970, PARCC, Université Paris Cité, Paris, France
[2] Poietis, Pessac, France
[3] Inserm UMR 1342, Centre d'investigation Clinique de Biothérapies CBT501, Paris, France
[4] Centre de L'oxygène R&D, Université de Liège, Sart-Tilman, Belgium
[5] Department of Cardiology, AP-HP, Hôpital Européen Georges Pompidou, Paris, France
[6] Department of Cardiovascular Surgery, AP-HP, Hôpital Européen Georges Pompidou, Paris, France

Introduction

Improved post-myocardial infarction (MI) survival has led to a rise in heart failure (HF) cases, highlighting the need for new treatments when the conventional ones fail. Cell therapy is one of those currently investigated and although the quest for the "ideal" cells continues, a great deal of interest is paid to mesenchymal stromal cells (MSC) as they may contribute to cardiac repair via angiogenic, anti-inflammatory, and immunomodulatory effects [1]. While the collection of MSC derived from bone marrow or adipose tissue require a fairly invasive

procedure, those from the umbilical cord are fraught with a substantial degree of lot-to-lot variability which makes challenging the yield of a consistent Advanced Therapy Medicinal Product. Thus, alternative sources of MSC still warrant further investigation. Among them, MSC from autologous skeletal muscle (mdMSC) have so far received less attention and there is not even a mention of this source in an extensive review of the diverse sources of MSC in the context of tissue regeneration [2] or in a recent compilation of MSC clinical trials [3]. However, their non-invasive collection via a microbiopsy procedure (Supplementary Fig. 1), their scalability (after 13,2 days ± 2,63 of culture, 15–20 mg of tissue yield ≈ 63,000 ± 30,675 cells) and the observation that they share with the other sources of MSC robust paracrinally-mediated cell-protective effects [4] provide a rationale to assess their potential relevance to cardiac repair.

This study was thus designed to first compare, in vitro, the effects of mdMSC with MSC from induced pluripotent stem cells (iPSC-MSC) as, in a clinical perspective, the latter also look attractive, in the perspective of a consistent product, because of their straightforward availability and their origin from a well-defined cell line. The most effective and safer candidate turned out to be the mdMSC which were then tested in a rat model of ischemia–reperfusion in combination with a bioprinted patch as, in a translational perspective, this material was deemed to be well suited for a scalable and reproducible clinical-grade manufacturing.

Results

MSC characterization

Flow cytometry was used to characterize iPSC-MSC and mdMSC, both of human origin. At passage 5, mdMSC expressed CD90, CD105, and CD73 (Fig. 1A) but no hematopoietic lineage markers (CD14, CD31, and CD45). In contrast, iPSC-MSC exhibited a complete absence of CD105 and partial loss of CD90, with only half of the population expressing it, while hematopoietic markers also remained undetected. The expression of pluripotency-related transcription factors, analyzed at passages 0 and 5, revealed the re-appearance over time of Sox2 and Oct3/4 within the iPSC-MSC population (Supplementary Fig. 2). A tri-lineage differentiation assay was then conducted (Fig. 1B). After several days of adipogenic induction, both MSC types exhibited specific morphological changes, including lipid vacuole accumulation. Chondrogenic and osteogenic differentiation was also confirmed using Alcian Blue and Alizarin Red S staining, respectively.

To further characterize MSC, their immunogenicity was assessed (Fig. 1C). iPSC-MSC dose-dependently inhibited T cell proliferation (left panel) while mdMSC were less immunosuppressive (right panel).

In vitro comparison of MSC

To evaluate the pro-angiogenic effects of MSC, a wound-healing assay was conducted on human umbilical vein endothelial cells (HUVEC). Incubation with iPSC-MSC and mdMSC significantly enhanced wound closure, with the effect becoming more pronounced as the MSC dose increased. Notably, mdMSC exhibited a stronger pro-angiogenic potential than iPSC-MSC (Fig. 2A).

A second potency assay tested MSC for their anti-apoptotic potential. The outcome measure was the viability of HUVEC following a one-hour exposure to staurosporine. Co-incubation with iPSC-MSC resulted in a small improvement in HUVEC viability, which was not found with mdMSC at the concentrations tested (Fig. 2C).

At the completion of this array of assays, the use of iPSC-MSC was considered problematic because of the re-appearance of some of the pluripotency-associated markers with the increased number of passages and their evaluation was thus discontinued because these transcription factors raised a risk of oncogenicity expected to hamper safe clinical applications. mdMSC, in contrast, were further assessed in vitro for their anti-fibrotic and anti-inflammatory properties. To this end, human cardiac fibroblasts (HCF) were first stimulated with TGF-β1, L-ascorbic acid and sulfate dextran which resulted in fibroblast activation (Fig. 3A). Incubation of HCF with

(See figure on next page.)

Fig. 1 Characterization of iPSC-MSC (left panel) and mdMSC (right panel). **A**: Flow cytometric analysis of iPSC-MSC at passage 3 (left) and mdMSC at passage 5 (right). MSC were stained for MSC and hematopoietic surface markers. mdMSC shown to express CD90, CD73, CD105, and no apparent CD45, CD14 and CD31. iPSC-MSC express CD73 only, and a third of the population also express CD90. Values show the percentage of positive cells (n = 3 biological replicates). **B**: Assays for iPSC-MSC (left) and mdMSC (right) differentiation. MSC were cultured with lineage-specific media to induce cell differentiation. Differentiation into adipocytes, osteocytes and chondrocytes was detected by oil Red O, alizarin red and alcian blue, respectively. Original magnification × 20 (n = 2 biological replicates). **C**: Effects of MSC on T-cell proliferation; a mixed lymphocyte reaction (MLR) was performed by co-culturing Peripheral Blood Mononuclear Cells (PBMC) labeled with the CellTrace™ Violet (CTV) Cell Proliferation Kit (Invitrogen) and the two types of MSC at different ratios; flow cytometry was then used for selecting T lymphocytes using anti-CD3 and anti-CD45 antibodies and 7AAD; the proliferation of the CTV-labeled selected lymphocyte proliferation was then fluorescently assessed (iPSC-MSC n = 1, mdMSC n = 3 biological replicates)

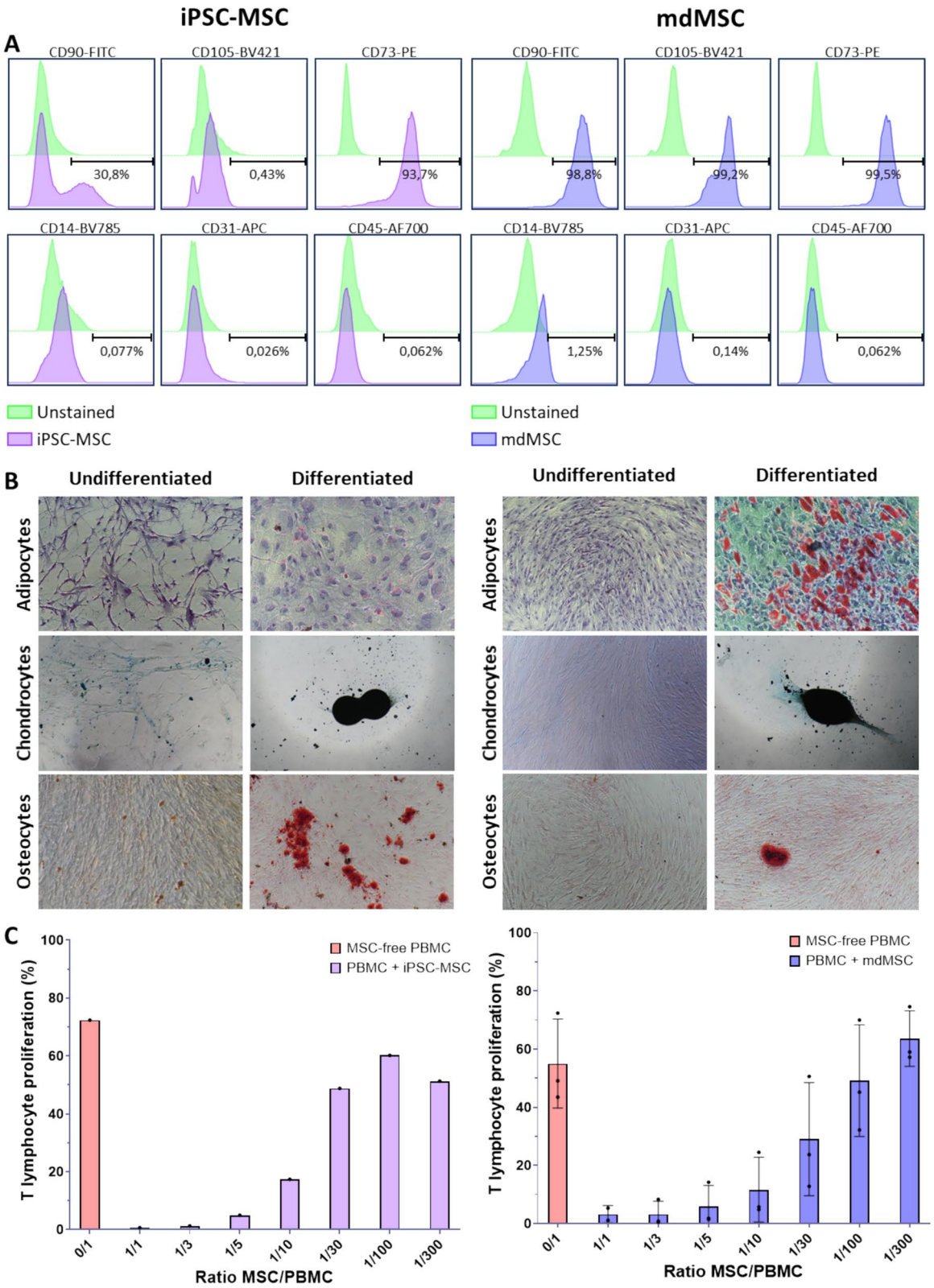

Fig. 1 (See legend on previous page.)

mdMSC led to a decrease in αSMA expression (Fig. 3B) taken as a read-out for an anti-fibrotic effect. This was further supported by PCR analysis, which revealed a significant downregulation of the fibrosis-associated genes *FN1* and *COL1A1*, while *POSTN*, *MMP2*, and *COL3A1* exhibited a similar downward trend (Fig. 3C). Finally, an inflammation assay was conducted using LPS-stimulated THP-1 monocytes. LPS stimulation followed by incubation with mdMSC resulted in a reduction of the pro-inflammatory cytokine TNFα compared to the LPS-only control (stimulated condition), paralleled by an increased secretion of the anti-inflammatory cytokine IL-10 (Fig. 3D). These findings are further supported by the analysis of the MSC secretome using a Luminex multiplex assay (Supplementary Fig. 5) performed under both basal conditions and after IFN-γ priming to simulate an inflammatory environment. The results revealed the secretion of several key cytokines with therapeutic potential. More specifically, Interleukin 6 (IL-6), known for its role in resolving inflammation and promoting myocardial repair post-infarction [5], was consistently expressed. Interferon γ-induced protein 10 (IP-10) was only detected after priming and is associated with improved left ventricular (LV) recovery and targeted immune modulation [6]. Monocyte chemoattractant protein 1 (MCP-1) secretion markedly increased under inflammatory conditions, and may play a role in recruiting pro-regenerative M2 macrophages [7]. Platelet-derived growth factor AA (PDGF-AA), may support post-infarction cardiac repair by enhancing angiogenesis and regulating fibroblast and inflammatory responses, was present at low levels and showed a slight decrease following priming [8, 9]. Finally, vascular endothelial growth factor (VEGF), a central angiogenic factor that supports neovascularization and enhances myocardial perfusion, was secreted steadily regardless of inflammatory stimulation [10, 11].

Put together, these in vitro data were considered encouraging enough to warrant proceeding to an in vivo assessment of mdMSC.

In vivo evaluation of the mdMSC-functionalized bioprinted collagen patch in a rat model of left ventricular dysfunction

Seventy immune-competent rats underwent a 45-min myocardial ischemia followed by reperfusion (Fig. 4A). Three weeks following the induction of MI, a baseline echocardiography was performed and only rats with a LV ejection fraction (LVEF) ≤ 60% were reoperated on and randomly assigned to one of the following three groups: sham (thoracotomy alone, n = 10), bioprinted a-cellular patch (n = 10), or bioprinted patch seeded with 100,000 mdMSC (n = 11). Bioprinting used acid-soluble bovine type I collagen as the bio-ink and was achieved by extrusion, which yielded a solid elastic hydrogel. Flow cytometry performed three days post-extrusion showed a high (> 90%) proportion of viable (calcein^{+}) cells. The patches were applied onto the epicardium of the heart with a hemostatic sponge (TachoSil®) placed at their outer surface and gently pressed to help the patch adhering to the heart. One month post-treatment, rats were re-assessed echocardiographically. All data were outsourced to a core laboratory when they were blindly analyzed. In both treatment groups, LV endsystolic volumes (LVESV) increased to a smaller extent from their respective baseline values (by 14.4 ± 9.6% in patch group and 9.1 ± 7.6% in patch + mdMSC group) than in sham group where they increased by 70.3 ± 16.8% (Fig. 4B). Left ventricular enddiastolic volumes (LVEDV) were also lower in the two patch-treated groups (Fig. 4C). As a result, LVEF declined from baseline by −7.6 ± 8.2% in the sham group; the patch-alone group showed an only minor decrease (− 3.2 ± 5.6%), while in the patch + mdMSC group LVEF improved by 14.4 ± 6.5% (Fig. 4D). In line with these findings, the stroke volume was significantly elevated in the patch + mdMSC group (Fig. 43E) where the enhanced cardiac function was further supported by the analysis of effect size which demonstrated the superiority of the cellularized patch over both its a-cellular counterpart and sham-operated controls (Supplementary Fig. 3). Infarct size did not differ among groups (Supplementary Fig. 4). A transcriptomic analysis of heart tissue was performed by RT-qPCR (Fig. 4F). Compared to the sham group, the patch + mdMSC group showed a significant reduction in the expression of genes associated with HF (*Ddah1*, *Nppb*), inflammation (*Cxcl11*, *Cxcl9*), and apoptosis (*Errfi1*). The patch-alone group also exhibited a downward trend in inflammatory markers.

(See figure on next page.)

Fig. 2 Potency assay evaluating MSC. **A**: Wound healing assay. Results of scar recolonization were normalized to the control poor medium. Data are presented as means ± SEM. p value: ≤ 0,05(*), ≤ 0.001(***), ≤ 0.0001(****) Ordinary one-way ANOVA with Dunnett's multiple comparisons test. **B**: Wound-heal photos under microscope at T0 et T24. Scale bars measure 1 mm. **C**: Viability test evaluating anti-apoptotic effects. Results were normalized to the control MP. Data are presented as means ± SEM. p value ≤ 0,05(*), ≤ 0.0001(****) Kruskal–Wallis test with Dunnett's multiple comparisons test

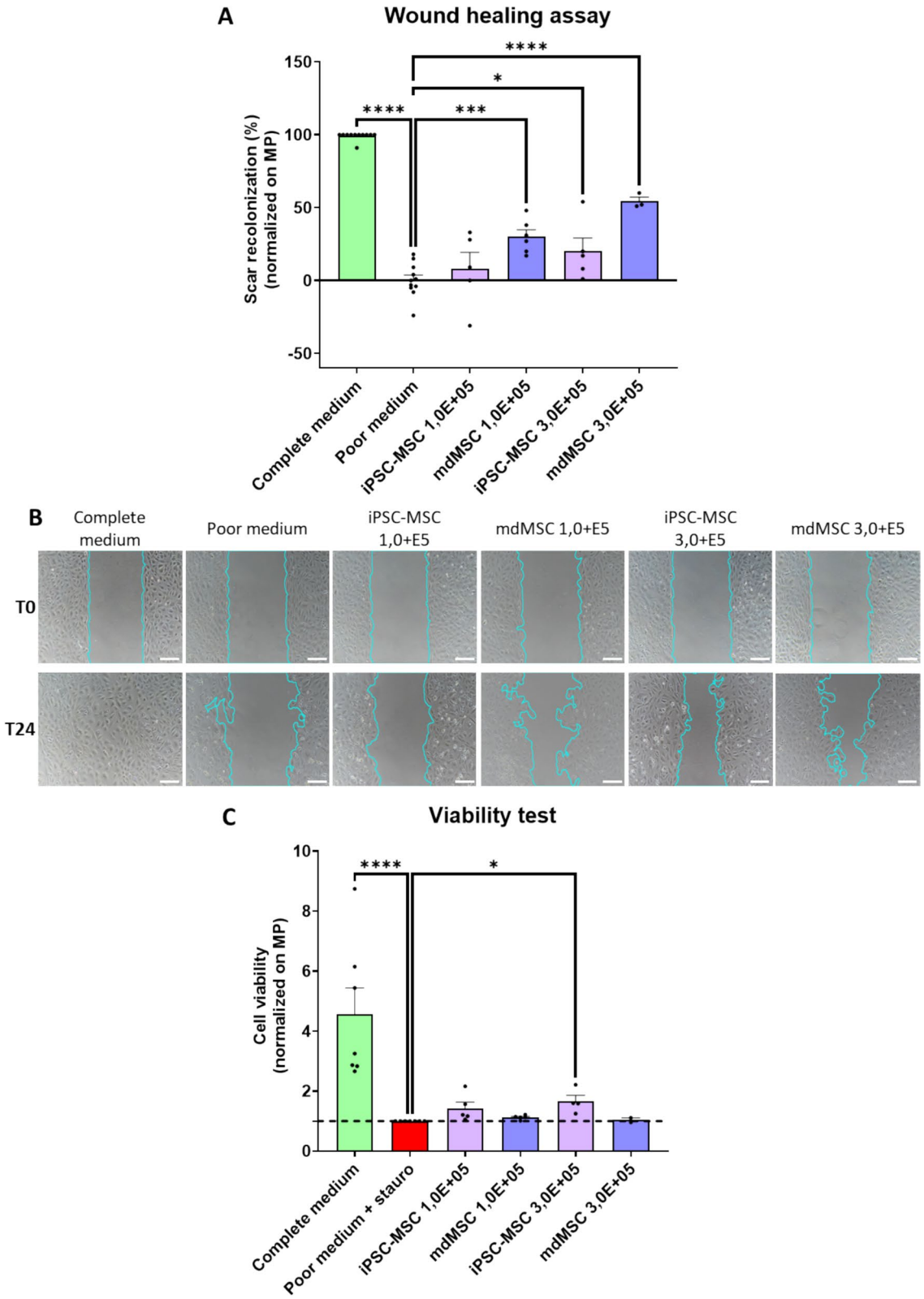

Fig. 2 (See legend on previous page.)

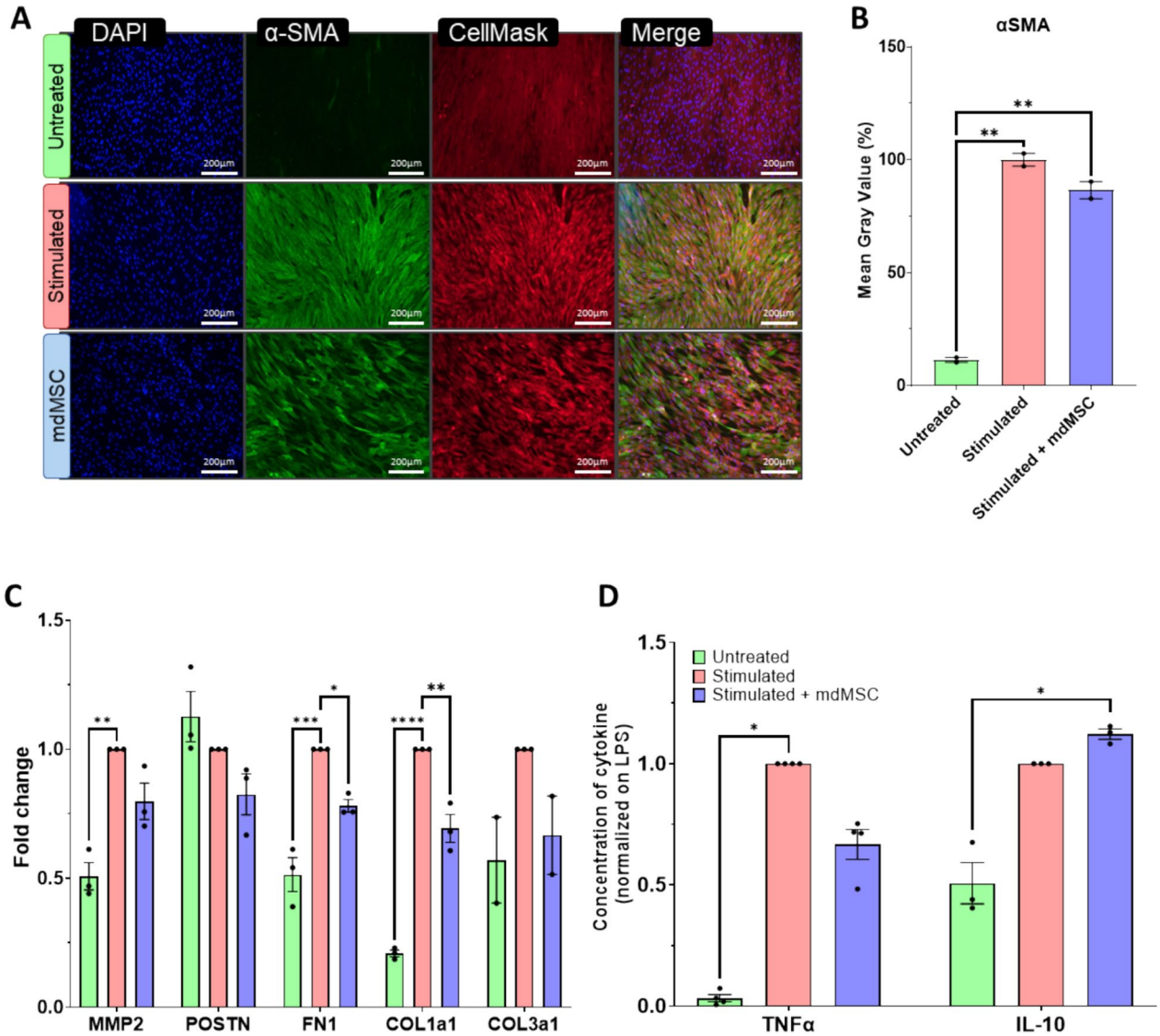

Fig. 3 Potency assay evaluating mdMSC. **A-B**: HCF imaging and quantification of mean fluorescence of αSMA. Scale bars measure 200 µm. Data are presented as means ± SEM. p value: ≤ 0.01(**) Ordinary one-way ANOVA with Dunnett's multiple comparisons test (n = 2 biological replicates). **C**: Expression of fibrosis-associated genes by HCF stimulated with TGF-β1, L-ascorbic acid and sulfate dextran. Data are presented as means ± SEM. p value: ≤ 0,05(*), ≤ 0,01(**), ≤ 0,001(***), ≤ 0,0001(****) Ordinary one-way ANOVA with Dunnett's multiple comparisons test. **D**: ELISA-based quantification of pro-inflammatory (TNFα) or anti-inflammatory (IL-10) cytokine production in THP-1 cells, with or without LPS stimulation. Data are presented as means ± SEM. p value: ≤ 0.05(*), Kruskal–Wallis test with Dunnett's multiple test correction

(See figure on next page.)

Fig. 4 In vivo evaluation of the mdMSC-loaded collagen patch in a rat model of left ventricular dysfunction. **A:** Experimental design. **B-E**: Changes in endsystolic (B) and enddiastolic (C) volumes and in LVEF (D) from baseline; Stroke Volume given in absolute values (E). Sham (n = 10), patch (n = 10), and patch + mdMSC (n = 11). Data are presented as means ± SEM. p value: ≤ 0.05(*), ≤ 0.01(**)—**B-C**: Ordinary one-way ANOVA with Dunnett's multiple test correction, **D**: Kruskal–Wallis test with Dunnett's multiple test correction, **E**: Repeated measures two-way ANOVA with Tukey's multiple test correction. **F**: Fold change in the expression of genes involved in apoptosis (Errfi1), inflammation (Cxcl11, Cxcl9), and heart failure (Nppb, Ddha1) in the three experimental groups: sham (n = 8), patch (n = 8), and patch + mdMSC (n = 9). Data are presented as means ± SEM. p value: ≤ 0.05(*) Kruskal–Wallis test with Dunnett's multiple test correction

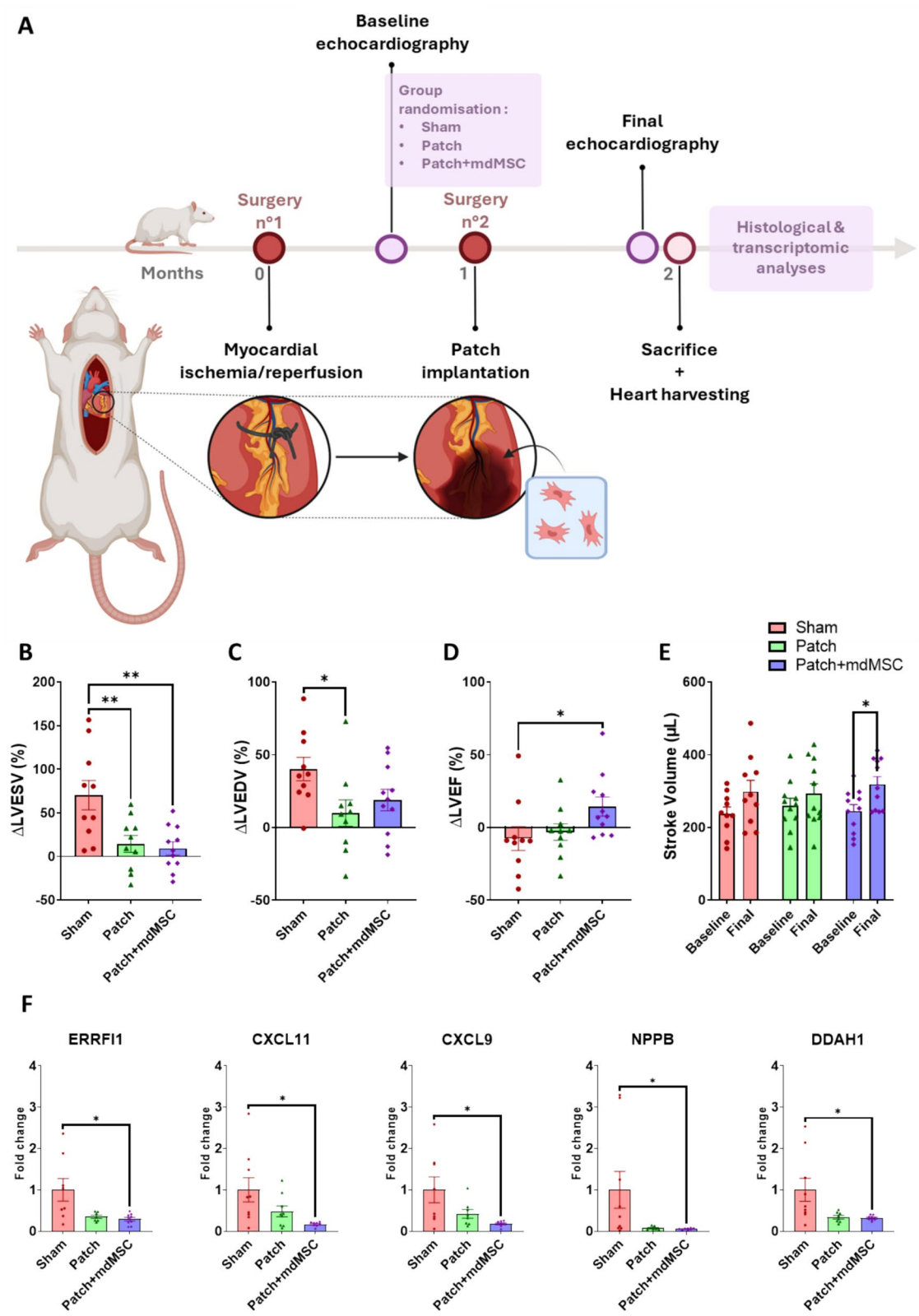

Fig. 4 (See legend on previous page.)

Discussion and conclusions

This study was driven by three clinically-oriented considerations: avoiding the immune response by using autologous cells; possibility to collect them by a minimally invasive procedure; and optimizing their engraftment by combining them with a scaffold. The integration of these three guidelines led us to assess the effects of mdMSC embedded in a bioprinted collagen patch.

While mdMSC share with the other main sources of autologous MSC (bone marrow and adipose tissue) a high scalability, they offer the distinct, clinically relevant advantage of a possible procurement by a minimally invasive procedure thanks to a unique muscle microbiopsy procedure (Supplementary Fig. 1) developed by Ceusters et al. [4, 12]. As a comparator, we selected iPSC-MSC which are also clinically attractive because their origin from a well-defined cell line along with a tight standardization of differentiation and expansion protocols are expected to yield a reproducible product [13]. However, we found that they did not fully match the whole set of criteria established by The International Society for Cellular Therapy (ISCT) in that they failed to fully express MSC-specific markers and, more noticeably, still demonstrated some of the iPSC-associated pluripotency factors [14]. The safety concern raised by the persistence of these markers [15] led us to privilege MSC from a muscular origin.

In our in vitro assays, these cells featured robust angiogenic and immune-modulatory effects. Of further relevance to the pathophysiology of the ischemic myocardium, mdMSC also demonstrated anti-fibrotic and anti-inflammatory properties in in vitro assays using stimulated fibroblasts and monocytes, respectively. Luminex analysis further confirmed the secretion of cytokines contributing to cardiac repair, with IFN-γ priming enhancing the secretion by mdMSC of IL-6, MCP-1, and IP-10, while VEGF remained consistently expressed regardless of any priming, supporting both immunomodulatory and pro-angiogenic functions.

These benefits were recapitulated in the in vivo model of chronic LV dysfunction where mdMSC improved the functional outcomes beyond those seen in the patch-alone group, thereby suggesting the cardio-protective effects of these cells possibly attributable to their paracrine effects demonstrated by the in vitro assays [5].

Beyond the nature of the cells, their mode of delivery is a critical factor of the ultimate outcome. Multiple intramyocardial injections have been initially used but their limitations are now recognized, which include needle-related damage to the cells; disruption of the extracellular matrix and subsequent loss of signals modulating cell survival and patterning; an inhomogeneous, difficult to standardize distribution; and the creation of potential arrhythmogenic clusters [16–18]. These hurdles can be overcome by the use of an epicardially delivered patch serving as a platform for the cells expected to act primarily though the release of paracrine mediators, without integration in the myocardium which is a safety net against arrhythmias. mdMSC were thus encapsulated in a collagen gel manufactured by bioprinting because this approach allows to carefully control the distribution of the cells while being amenable to a standardized large-scale production [19, 20]. Indeed, the naked collagen patch yet provided some degree of cardiac preservation compared with sham-operated rats, in line with the well-documented benefits of collagen [21, 22], but the patch-associated improvement in the functional outcomes was further enhanced when the collagen bioink was combined with the mdMSC, suggesting a synergistic effect of the cells and the hydrogel. This result aligns with previous reports documenting the benefits of diverse combinations of cells and bioinks: progenitor cardiac cells in a mix of gelatin and hyaluronic acid [23]; progenitor cardiac cells and MSC in a decellularized extracellular matrix [24, 25]; and even iPSC-derived cardiomyocytes, endothelial cells and fibroblasts clustered in bioprinted scaffold-free cardiospheres [26]. That the bioprinted patch improved function without significantly reducing infarct size is not an uncommon observation as cardiac function and the macroscopic size of cardiac scars have previously been shown to be possibly uncoupled readouts [27]. Indeed, one month post-infarction, the fibrotic scar is already fixed, and any functional improvement is expected to be mainly due to the preservation of the still viable myocardium mediated by the paracrine effects of both the transplanted cells and the collagen biomimetic properties, as suggested by our transcriptomic data collected following implantation of both cellular and acellular patches.

In summary, this study does not claim the superiority of mdMSC over the other commonly used MSC but suggests that these cells may enrich the landscape of cardiac cell therapy by providing an attractive source of autologous cells retrievable by a minimally invasive harvesting method. Bioprinting mdMSC with a biocompatible material with a long-standing safety record like collagen allowed the straightforward production of a clinically usable patch endowed with cardio-reparative properties.

Materials and methods

iPSC-MSC cell culture

Cryopreserved iPSC-derived MSC (iCell® Mesenchymal Stem Cells, FUJIFILM Cellular Dynamics International, Inc, WI, États-Unis) are thawed and seeded at a density of 35,000 cells/cm^2 in RoosterNourish™-CSM-XF culture medium (RoosterBio, Frederick, MD, États-Unis)

supplemented with 1% antimycotic antibiotic solution (Sigma-Aldrich, Saint-Louis, MO, États-Unis). The cells are then placed in an incubator at 37 °C and 5% CO_2. The medium is changed every 6 days until the cells reach 80% confluence (passage 0). The cells are then detached with trypsin–EDTA (ThermoFisher, Waltham, MA, États-Unis) collected and reseeded at a density of 5,000 cells/cm^2 up to passage 2 to build up a bank.

mdMSC cell culture

Cryopreserved MSC are thawed and seeded at a density of 35,000 cells/cm^2 in MesenCult™ Proliferation Kit culture medium (StemCell, Vancouver, BC, Canada) supplemented with 1% antimycotic antibiotic solution (Sigma-Aldrich). Cells are then placed in an incubator at 37 °C and 5% CO_2. The medium is changed the day after thawing, then every 2 days until the cells reach 80% confluence (passage 4). Cells are then detached with TrypLE™ Express (ThermoFisher), collected and reseeded at a density of 5,000 cells/cm^2 up to passage 2 to build up a bank.

Flow cytometry characterization of MSC

MSC were analyzed by flow cytometry using surface markers CD90 (FITC, clone 5A10, Biolegend, San Diego, CA, États-Unis), CD105 (BV421™, clone 43A3, Biolegend), and CD73 (PE, clone AD2, Biolegend). Hematopoietic markers CD14 (BV786, clone M5E2, BD Biosciences), CD45 (AF700, clone 2D1, Biolegend), CD31 (APC, clone WM59, Biolegend), and HLA-DR (PE/Cy7, clone L243, Biolegend) were used to confirm their absence. Negative controls included unstained MSCs and PBMCs.

iPSC-MSC were stained for Nanog (Vio B515, clone REA314, Miltenyi Biotec), Sox2 (PE, clone REA320, Miltenyi Biotec, Bergisch Gladbach, Allemagne), and Oct3/4 (APC, clone REA622, Miltenyi Biotec) using the Transcription Factor Staining Buffer Set (Miltenyi Biotec), following the manufacturer's protocol. Controls included unstained iPSC-MSC and iPSC.

Samples were acquired using a LSRFortessa™ X-20 cytometer (BD Biosciences) and analyzed with FlowJo v10.10.0 (BD Biosciences).

Differentiation into chondrocytes, adipocytes and osteocytes

The ability of MSC to differentiate into adipocytes, chondrocytes and adipocytes was assessed using the following kits: StemPro® Adipogenesis Differentiation Kit (ThermoFisher), StemPro® Chondrogenesis Differentiation Kit (ThermoFisher), StemPro® Osteogenesis Differentiation Kit (ThermoFisher). These kits were used according to the supplier's recommendations.

Mixed lymphocyte reaction

The immunosuppressive capacity of mdMSC and iPSC-MSC was assessed using a mixed lymphocyte reaction (MLR) assay adapted from Nicotra et al. (28). MSC were pretreated with IFN-γ for 48 h prior to co-culture. PBMC from 10 healthy donors were labeled with CellTrace™ Violet Cell Proliferation Kit (Invitrogen) and co-cultured with MSC at ratios of 0:1 (control), 1:1, 1:3, 1:5, 1:10, 1:30, 1:100, and 1:300 (MSC:PBMC). Cells were cultured in RPMI 1640 medium supplemented with GlutaMAX™, HEPES (ThermoFisher), 10% human AB serum (Eurobio, Les Ulis, France), 1% Amphotericin B/Penicillin/Streptomycin (ThermoFisher), and 10 IU/mL Heparin (PanPharma, Luitré, France), at 37 °C with 5% CO_2. On day 4, 50 µL of fresh medium was added. On day 7, cells were stained with anti-human CD3-PE (BD Biosciences), CD45-FITC (BD Biosciences), and viability dye 7-AAD (Beckman Coulter, Villepinte, France) for 15 min at 4 °C in the dark.

Cells were washed with PBS and analyzed using an Attune NxT™ Flow Cytometer (ThermoFisher), and data were processed with Attune NxT™ software.

Scratch test

Human umbilical vein endothelial cells (HUVEC, Promocell, Heidelberg, Allemagne) at early passages (P2–P6) are seeded at 40,000 cells/well in 2-well culture inserts (Ibidi GmbH, Munich, Germany) placed in 24-well plates with Endothelial Cell Growth Medium (Promocell) supplemented with 1% antibiotic–antimycotic (Sigma-Aldrich), and incubated at 37 °C with 5% CO_2.

In parallel, iPSC-MSC and mdMSC are seeded at 100,000 or 300,000 cells/well in 6.5 mm Transwell® inserts (0.4 µm pore, Corning, Kennebunk, ME, USA), in RoosterNourish™-CSM-XF medium (RoosterBio) and MesenCult™ medium (StemCell) respectively, and incubated under the same conditions for 24 h.

Once HUVEC reach confluence, inserts are removed to create a 500 µm wound. Wells are then filled with:

- Positive control: complete medium (basal + 10% FBS)
- Negative control: basal medium only
- MSC condition: basal medium + MSC in Transwell

Images are taken at T0 and T24 h, and wound closure is assessed by comparing the cell-free area between both time points.

Viability test

Wells of a 24-well plate are coated with 0.1% gelatin. HUVEC (Promocell, passages 2–6) are seeded at 90,000

cells/well in Endothelial Cell Growth Medium (Promocell) supplemented with 1% antibiotic–antimycotic solution (Sigma-Aldrich).

In parallel, iPSC-MSC and mdMSC are seeded at 100,000 or 300,000 cells/well in 6.5 mm Transwell® inserts (0.4 µm pores, Corning) using RoosterNourish™-CSM-XF (RoosterBio) or MesenCult™ (StemCell) media, respectively, each supplemented with 1% antibiotic–antimycotic. All cells are incubated at 37 °C, 5% CO_2 for 24 h.

The next day, HUVECs are treated with 0.05 µM staurosporine (Cell Signaling Technology, Danvers, MA, USA) in basal medium (without supplements) for 1 h, then gently rinsed twice. Wells are then filled with:

- Positive control: complete medium (basal + 10% FBS)
- Negative control: basal medium
- MSC condition: basal medium with Transwell inserts containing MSC

After 24 h, cell viability is assessed using the CCK-8 assay (Sigma-Aldrich, 1:10 dilution, 3 h incubation at 37 °C). Absorbance at 450 nm is measured using a SPECTROstar Nano spectrophotometer (BMG LABTECH, Ortenberg, Allemagne), and data are analyzed with MARS software. Results are normalized to the negative control.

Multiplex cytokine quantification

Conditioned media were collected from mdMSC cultured for 24 h in poor medium (without FBS), with or without IFN-γ stimulation (20 ng/mL). Supernatants were clarified by centrifugation at 400 × g for 5 min and stored at –80 °C until analysis.

Cytokine concentrations were measured using the Human XL Cytokine Luminex® Performance Assay 46-plex Fixed Panel (R&D Systems, Bio-Techne, Minneapolis, MN, USA), following the manufacturer's protocol. Plates were read on a Luminex® 200 system (Luminex Corporation, Austin, TX, USA), and data were analyzed with xPONENT software (v4.2). Cytokine levels were calculated from standard curves, and all samples were run in triplicate.

Anti-fibrotic assay

Human cardiac fibroblasts (HCF, Promocell, passages 1–5) are cultured in Fibroblast Growth Medium 3 (Promocell) supplemented with 1% antibiotic–antimycotic solution (Sigma-Aldrich) at 37 °C, 5% CO_2 until 80% confluence. Cells are then seeded at 30,000 cells/cm^2 in 24-well plates and incubated for 24 h. The medium is replaced with a deprivation medium (DM) (DMEM high glucose, 0.5% FBS, 1% antibiotic–antimycotic, 1% non-essential amino acids) for 24 h. Next, cells are stimulated for 24 h in a stimulation medium (DM, 100 µM L-ascorbic acid 2-phosphate, 10 ng/mL TGF-β1, 100 µg/mL dextran sulfate). In parallel, mdMSC are seeded at 100,000 or 300,000 cells/well in 6.5 mm Transwell® inserts (0.4 µm pores, Corning) using MesenCult™ medium (StemCell) supplemented with 1% antibiotic–antimycotic, and incubated for 24 h. After stimulation, HCF and mdMSC cultures are rinsed with deprivation medium, and Transwells are placed into the HCF wells (stimulated + mdMSC) for 24 h of indirect coculture at 37 °C. Finally, Transwells are removed and HCF are either fixed for immunofluorescence or collected after trypsinization and stored at −80 °C for qPCR analysis.

Immunofluorescence

HCF are fixed with 2% paraformaldehyde for 15 min at 37 °C, then washed with cold PBS. Permeabilization and blocking are performed for 1 h at 37 °C in PBS containing 10% FBS and 0.2% Triton X-100. Cells are incubated overnight at 4 °C with anti-α-SMA primary antibody (clone 1A4, Sigma-Aldrich), then for 1 h at room temperature with Alexa Fluor™ 488-conjugated secondary antibody (ThermoFisher) and CellMask™ Deep Red. Nuclei are stained with DAPI for 3 min. Images are acquired using a Leica DM6000 inverted microscope and analyzed with ImageJ.

RNA extraction, RT-PCR and PCR

Total RNA is extracted using the RNeasy kit (Qiagen, Hilden, Allemagne) and quantified with a NanoDrop™ One spectrophotometer (ThermoFisher). cDNA is synthesized using the QuantiTect Reverse Transcription Kit (Qiagen). qPCR is performed in 96-well plates using SYBR® Green reagents (Meridian Bioscience, Cincinnati, OH, USA) on a StepOnePlus thermal cycler (ThermoFisher). GAPDH is used as the housekeeping gene. Primers are designed with Oligo 7 software; sequences and annealing temperatures are provided below. Results are normalized to the negative control (stimulated) (Table 1).

Anti-inflammatory assay

mdMSC are seeded at 300,000 cells/well in 6.5 mm Transwell® inserts (0.4 µm pores, Corning) with MesenCult™ medium (StemCell), 10% FBS, and 1% antibiotics, and incubated for 24 h at 37 °C, 5% CO_2. The next day, THP-1 monocytes are seeded at 100,000 cells/cm^2 in RPMI 1640 complete medium (10% FBS, 1% PSA) and stimulated with 1 µg/mL of lipopolysaccharide (LPS), except for the untreated control. Transwells containing mdMSC are rinsed and transferred into THP-1 wells (stimulated + mdMSC) for 24 h of indirect co-culture. Supernatants are collected, centrifuged, aliquoted, and

Table 1 List of human primers for qPCR

Species	Gene	F/R	Sequence (5'to 3')	Hybridization temperature	Role
Human	*COL1A1*	Forward	GCACCTGCCGTGACCTCAAGAT	64,2°C	Fibrosis
		Reverse	TGGCCGCCATACTCGAACTGGAAT		
	COL3A1	Forward	ATCAGGCCAGTGGAAATGTAAAGA	59,8°C	Fibrosis
		Reverse	TCACAGCCTTGCGTGTTCGATAT		
	FN1	Forward	TCCCATTATGCCGTTGGAGATGAG	59,8°C	Fibrosis
		Reverse	ICAICIGGCCAI 1 1 ICICCCIGAC		
	GAPDH	Forward	ATGGGGAAGGTGAAGGTCGGAG	60°C	Housekeeping gene
		Reverse	TCGCCCCACTTGATTTTGCAGG		
	MMP2	Forward	GCGAGTGGATGCCGCCTTTAACTG	61,5°C	Matrix degradation/ Cardiac remodeling
		Reverse	GTCCACGACGGCATCCAGGTTATC		
	POSTN	Forward	GGAGAAACGGTGCGATTCACATAT	59,4°C	Cardiac remodeling
		Reverse	AGAGCAI I I I IGICCCGIAICAGA		

stored at −80 °C. TNFα and IL-10 levels are measured by ELISA (Biotechne, MN, États-Unis) according to the manufacturer's protocol, and optical density is read at 450/570 nm.

Transcriptomic analysis of hearts

Total RNA is extracted from cardiac tissue using TRIzol™ (Invitrogen, Waltham, MA, États-Unis) following the manufacturer's protocol. RNA concentration and purity are measured with a NanoDrop™ One spectrophotometer (ThermoFisher), and reverse transcription is performed using the QuantiTect Reverse Transcription Kit (Qiagen). Gene expression related to fibrosis, apoptosis, and heart failure is analyzed using the same RT-qPCR protocol described in the "**RNA extraction, RT-PCR and PCR**" section. Primer sequences and annealing temperatures are listed in the table below. Results are normalized to the sham group (Table 2).

Experimental model

Seven-week-old male immunocompetent Wistar rats (approximately 200 g) were obtained from Janvier Labs. They were housed in our animal facility under specific pathogen-free conditions, with free access to food and water, and maintained on a 12-h light/12-h dark cycle. Rats were housed three per cage initially, and reduced to two per cage once they exceeded 300 g. Each cage was equipped with environmental enrichment items, including wooden chew blocks, shelters, and nesting substrates. In this study, the experimental unit is the individual animal, as *n* corresponds to the number of animals used.

The required sample size was calculated based on a two-sided test with a significance level (α) of 0.05 and a statistical power (1 − β) of 0.80, assuming a standard deviation (σ) of 10. Using the formula:

$$n = \frac{2 \times \left(Z_{\alpha/2} + Z_{\beta}\right)^2 \times \sigma^2}{\Delta^2}$$

where $\Delta = 13$ is the minimal biologically significant difference in LV ejection fraction to detect,$Z_{\alpha/2} = 1.96$, and$Z_{\beta} = 0.84$, the estimated sample size per group is:

$$n = \frac{2 \times (1.96 + 0.84)^2 \times 10^2}{13^2} = 9.27$$

Therefore, at least 10 animals per group are required to reliably detect a 13-unit difference under these assumptions and our sample sizes have met these numbers.

Experimental procedures

Procedures

The first procedure is performed to induce myocardial ischemia–reperfusion injury in rats, thereby establishing the heart failure model. A total of 70 rats were included. Twelve rats died during surgery. Cardiac function was assessed by echocardiography three weeks after infarction to evaluate the severity of injury. At this stage, 27 rats were excluded due to a left ventricular ejection fraction (LVEF) greater than 60%, and 31 rats were included and randomly assigned to one of the following three groups: sham (n = 10), patch (n = 10), or patch + mdMSC (n = 11). Randomization was performed using Microsoft Excel, with the aim of ensuring a homogeneous distribution of LVEF values across the three groups. The sham group, which underwent thoracotomy alone without coronary artery encircling or any additional treatment, served as the control group. The treatment was administered via a re-thoracotomy for patch implantation with or without cells three weeks after the index injury. An hemostatic sponge (TachoSil®) was applied at the outer surface of the patch and gently pressed against the myocardial tissue

Table 2 List of rat primers for qPCR

Species	Gene	F/R	Sequence (5′ or 3′)	Hybridization temperature	Role
Rat	*Col1a1*	Forward	AGCATGTCTGGTTTGGAGAG	60°C	Fibrosis
		Reverse	GTGATAGGTGATGTTCTGGGAG		
	Col3a1	Forward	GTGAACATGGCCCTCCAG	60°C	Fibrosis
		Reverse	CCTCTTTCTCCTTTAGCACCTG		
	Cxcl9	Forward	CAAACCTGCCTAGACCCAGATTCA	59,6°C	Inflammation
		Reverse	GACTCCGGATGGTGGGGTGTTTTA		
	Cxclll	Forward	ACGGTTCCAGGCTTCGTTATGTTC	59,6°C	Inflammation
		Reverse	GGTCCAGGCACCTTTGTCCTTTAT		
	Ddahl	Forward	GCTGGCCCCAACCTGATCGCAATA	62,2°C	Cardiac function
		Reverse	CGTCCGGTACAGTGAGCTTGTCAT		
	Errfil	Forward	GCC GTTTCTGGACCATGTTATCTA	60,1°C	Apoptosis
		Reverse	CACCCCACGATAACTCTCAATCAT		
	Fnl	Forward	GGTACCACTGGCCACACCTACAAC	59,6°C	Fibrosis
		Reverse	GCACGTCCAACGGCATGAAGCATT		
	Gapdh	Forward	GGGCTCTCTGCTCCTCCCTGTTCT	63,7°C	Housekeeping gene
		Reverse	TCACAAGAGAAGGCAGCCCTGGTA		
	Ly6c	Forward	TGTGCAGAAAGAGCTCAGGGCTTA	60°C	Inflammation
		Reverse	ACAGAGCCCTCTACAGCTTCTAAC		
	Nppb	Forward	CGGGCIGAGGI IGII 1 IAGGAAGA	59,2°C	Heart failure
		Reverse	GGCAAGTTTGTGCTGGAAGATAAG		
	Plod2	Forward	TCCGGCCTCACCACGATGCGTCAA	62,5°C	Fibrosis
		Reverse	CGGGGGGATTCGATGGAGCAATTA		
	Postn	Forward	ATAGACGGGGTTCCTGTTGAAATA	59,2°C	Cardiac remodeling
		Reverse	TGATCGCCTTCTAGACCCTTGAAC		
	Ptgs2	Forward	TCTGGTGCCGGGTCTGATGATGTA	62,5°C	Inflammation
		Reverse	CGCTCAGGTGTTGCACGTAGTCTT		
	Thbsl	Forward	TACCAGTCCAGCAGCCGCTTCTAC	62,8°C	Cardiac remodeling
		Reverse	CGGGGCCAGTGGTGGAGTTTACAA		

with a gauze dressing to allow the patch to adhere, which only took a few minutes. One month after treatments, cardiac function was reassessed by echocardiography, and the animals were euthanized for heart collection.

All echocardiographic measurements were performed in a randomized order (based on the position of the cages on the rack) to avoid introducing bias into the assessments. All data were analyzed in a blinded manner by an independent core laboratory, which assessed the following parameters: left ventricular ejection fraction (LVEF), left ventricular end-diastolic volume (LVEDV), left ventricular end-systolic volume (LVESV), and stroke volume. Data were double-checked by a senior echocardiographist (A.H.).

Anaesthesia and euthanasia

All procedures were performed under inhalation anesthesia with 2.5% isoflurane. During surgical procedures, rats were placed on a heating pad and provided with an ocular lubricant (Lubrithal).

Analgesia protocol: pre-operative and post-operative buprenorphine injections (0.05 mg/kg) were administered for 48 h, and lurocaïne® was injected at the incision site at the beginning and end of the procedure.

After the second echocardiography, all animals were euthanized using deep inhalation anesthesia with 5% isoflurane. The heart, which had to remain intact, i.e., still beating at the time of harvesting, was collected for histological and transcriptomic analyses.

Statistical methods

Data are presented as means ± standard error of the mean (SEM).

Statistical analyses were conducted using Prism 10.0 software (GraphPad Software, San Diego, CA, USA). For both in vitro and in vivo experiments, data with a normal distribution were analyzed using one-way

analysis of variance (ANOVA) followed by Dunnett's post hoc test. Non-normally distributed data were assessed using the Kruskal–Wallis test for multiple comparisons. An effect size was also determined using the following equation:

$$d = \frac{\overline{x}_1 - \overline{x}_2}{\sigma_{\text{pooled}}}$$

$\overline{x}_1$: mean of group 1, $\overline{x}_2$: mean of group 2, σ_{pooled}: pooled standard deviation of the two groups, calculated using the following formula:

$$\sigma_{\text{pooled}} = \sqrt{\frac{(n_1 - 1) \times \sigma_1^2 + (n_2 - 1) \times \sigma_2^2}{n_1 + n_2 - 2}}$$

n_1: sample size of group 1, n_2: sample size of group 2,σ_1: standard deviation of group 1, σ_2: standard deviation of group 2.

Abbreviations

EV	Extracellular vesicle
HCF	Human cardiac fibroblasts
HF	Heart failure
HUVEC	Human umbilical vein endothelial cell
IL-10	Interleukin 10
IL-6	Interleukin 6
IP-10	Interferon γ-induced protein 10
iPSC	Induced pluripotent stem cells
iPSC-MSC	IPSC derived mesenchymal stromal cell
LPS	Lipopolysaccharide
LV	Left ventricular
LVEDV	Left ventricular ejection diastolic volume
LVEF	Left ventricular ejection fraction
LVESV	Left ventricular ejection systolic volume
MCP1	Monocyte chemoattractant protein 1
mdMSC	Muscle derived mesenchymal stromal cell
MI	Myocardial infarction
MSC	Mesenchymal stromal cell
PDGF AA	Platelet-derived growth factor AA
TNFα	Tumor necrosis factor α
VEGF	Vascular endothelial growth factor
αSMA	α-Smooth muscle actin

Supplementary Information

The online version contains supplementary material available at https://doi.org/10.1186/s13287-025-04552-7.

Additional file 1.

Acknowledgements
The authors would like to thank Gilles Renaud and Franck Lager from the Institut Cochin Life Imaging Platform for their assistance with the analysis of echocardiographic data.

Author contributions
R.G. and P.M designed the protocol analyzed data, and drafted the manuscript. R.G., S.S., A.C. and E.P. conducted experiments and acquired data. D.S. and J.C. developed the microbiopsy harvest procedure and took care of mdMSC collection and production. A.H. assessed and validated the echocardiographic data. F.G. provided scientific advice and reviewed the manuscript. All the authors contributed to the final manuscript.

Funding
This project was funded under the "Conventions Industrielles de Formation par la REcherche" (CIFRE) program, with the support of the company Poietis.

Availability of data and materials
The datasets generated during and/or analyzed during the current study are available from the corresponding authors.

Declarations

Human or animal rights
The mdMSC were obtained from the company REVATIS following the establishment of a Material Transfer Agreement. Human samples are derived from healthy volunteer donors who provided an informed consent. All experiments are approved by the Regional Ethical Research Committee of the Bordet Institute and conducted in accordance with the principles outlined in the Declaration of Helsinki [4]. The T-cells were obtained from PBMC in AP-HP, Hôpital Saint-Louis, Unité de Thérapie Cellulaire. All samples collected from healthy adult donors were obtained after a written and informed consent, following the Helsinki's Declaration and in compliance with the regulation of the Health Authorities. Approval was obtained from the Comité de Protection des Personnes (Ethics Committee) Ile de France IV (IRB00003835) [28]. The iPSC-MSC (iCell Mesenchymal Stem Cells Kit, 01279 #R1098) were purchased from FUJIFILM Cellular Dynamics, Inc. (FCDI). The original iPSC lines were sourced from the CIRM iPSC Repository, which contains samples from 2,500 donors. All tissue collection and informed consent procedures were conducted in accordance with CIRM guidelines and approved by Institutional Review Boards. The Human Umbilical Vein Endothelial Cells (HUVEC, #C-12200) and Human Cardiac Fibroblasts (HCF, #C-12375) were purchased from PromoCell and obtained from donors who have signed an informed consent form detailing the purpose of the donation and the tissue processing procedure. All procedures were approved by the Institutional Ethics Committee from the Université de Paris (Project APAFIS#25824) on the 19/08/2020 and comply with the ARRIVE guidelines 2.0 and with the European legislation (EU Directive 2010/63/EU for animal experiments). All procedures followed approved ethical guidelines and institutional policies. The project title is: "Évaluation des vésicules extracellulaires dérivées de cellules souches d'origine humaine comme une alternative à la greffe des cellules: applications à la réparation myocardique dans un modèle d'insuffisance cardiaque chronique avec validation du biomatériau chez le rat." For this paper, we have only used the stem cell component of the application (and not the extracellular vesicles).

Competing interests
D.S. and J.C. are scientific advisors of Revatis, a Spin Off company of the University of Liege.

Received: 17 April 2025 Accepted: 18 July 2025
Published online: 05 August 2025

References

1. Guo Y, Yu Y, Hu S, Chen Y, Shen Z. The therapeutic potential of mesenchymal stem cells for cardiovascular diseases. Cell Death Dis. 2020;11(5):349.
2. Brown C, McKee C, Bakshi S, Walker K, Hakman E, Halassy S, et al. Mesenchymal stem cells: cell therapy and regeneration potential. J Tissue Eng Regen Med. 2019;13(9):1738–55.
3. Jovic D, Yu Y, Wang D, Wang K, Li H, Xu F, et al. A brief overview of global trends in MSC-based cell therapy. Stem Cell Rev Rep. 2022;18(5):1525–45.
4. Ceusters J, Lejeune JPh, Sandersen C, Niesten A, Lagneaux L, Serteyn D. From skeletal muscle to stem cells: an innovative and minimally-invasive process for multiple species. Sci Rep. 2017;6(7):696.
5. Zhu H, Liu X, Ding Y, Tan K, Ni W, Ouyang W, et al. IL-6 coaxes cellular dedifferentiation as a pro-regenerative intermediate that contributes to pericardial ADSC-induced cardiac repair. Stem Cell Res Ther. 2022;13(1):44.
6. Sopova K, Tual-Chalot S, Mueller-Hennessen M, Vlachogiannis NI, Georgiopoulos G, Biener M, et al. Effector T cell chemokine IP-10 predicts cardiac recovery and clinical outcomes post-myocardial infarction. In:

Front Immunol [Internet]. 2023 Jun 22 [cited 2025 Jun 27];14. Available from: https://www.frontiersin.org/journals/immunology/articles/https://doi.org/10.3389/fimmu.2023.1177467/full
7. Niu J, Kolattukudy PE. Role of MCP-1 in cardiovascular disease: molecular mechanisms and clinical implications. Clin Sci. 2009;117(3):95–109.
8. Medamana J, Clark RA, Butler J. Platelet-Derived Growth Factor in Heart Failure. In: Bauersachs J, Butler J, Sandner P, editors. Heart failure [Internet]. In: Cham: Springer International Publishing; 2016 [cited 2025 Jun 29]. p. 355–69. (Handbook of Experimental Pharmacology; vol. 243). Available from: http://link.springer.com/https://doi.org/10.1007/164_2016_80
9. Zhao W, Zhao T, Huang V, Chen Y, Ahokas RA, Sun Y. Platelet-derived growth factor involvement in myocardial remodeling following infarction. J Mol Cell Cardiol. 2011;51(5):830–8.
10. Zisa D, Shabbir A, Suzuki G, Lee T. Vascular endothelial growth factor (VEGF) as a key therapeutic trophic factor in bone marrow mesenchymal stem cell-mediated cardiac repair. Biochem Biophys Res Commun. 2009;390(3):834–8.
11. Markel TA, Wang Y, Herrmann JL, Crisostomo PR, Wang M, Novotny NM, et al. VEGF is critical for stem cell-mediated cardioprotection and a crucial paracrine factor for defining the age threshold in adult and neonatal stem cell function. Am J Physiol-Heart Circ Physiol. 2008;295(6):H2308–14.
12. Serteyn D, Ceusters J. New uses of mammalian muscle-derived stem cells [Internet]. US20210116441A1, 2021 [cited 2025 Apr 14]. Available from: https://patents.google.com/patent/US20210116441A1/fr
13. Khan MA, Alanazi F, Ahmed HA, Shamma T, Kelly K, Hammad MA, et al. iPSC-derived MSC therapy induces immune tolerance and supports long-term graft survival in mouse orthotopic tracheal transplants. Stem Cell Res Ther. 2019;10(1):290.
14. Choudhery MS, Mahmood R, Harris DT, Ahmad FJ. Minimum criteria for defining induced mesenchymal stem cells. Cell Biol Int. 2022;46(6):986–9.
15. Zhao C, Ikeya M. Generation and Applications of Induced Pluripotent Stem Cell-Derived Mesenchymal Stem Cells. Stem Cells Int. 2018;2018:9601623.
16. van den Akker F, Feyen DAM, van den Hoogen P, van Laake LW, van Eeuwijk ECM, Hoefer I, et al. Intramyocardial stem cell injection: go(ne) with the flow. Eur Heart J. 2017;38(3):184–6.
17. Fukushima S, Varela-Carver A, Coppen SR, Yamahara K, Felkin LE, Lee J, et al. Direct intramyocardial but not intracoronary injection of bone marrow cells induces ventricular arrhythmias in a rat chronic ischemic heart failure model. Circulation. 2007;115(17):2254–61.
18. Aguado BA, Mulyasasmita W, Su J, Lampe KJ, Heilshorn SC. Improving viability of stem cells during syringe needle flow through the design of hydrogel cell carriers. Tissue Eng Part A. 2012;18(7–8):806–15.
19. Silva LP. Current trends and challenges in biofabrication using biomaterials and nanomaterials: future perspectives for 3D/4D bioprinting. In: 3D and 4D printing in biomedical applications [Internet]. John Wiley & Sons, Ltd; 2019 [cited 2021 Oct 5]. p. 373–421. Available from: https://onlinelibrary.wiley.com/doi/abs/https://doi.org/10.1002/9783527813704.ch15
20. Derakhshanfar S, Mbeleck R, Xu K, Zhang X, Zhong W, Xing M. 3D bioprinting for biomedical devices and tissue engineering: a review of recent trends and advances. Bioact Mater. 2018;3(2):144–56.
21. Muthukumar T, Sreekumar G, Sastry TP, Chamundeeswari M. Collagen as a potential biomaterial in biomedical applications. Rev Adv Mater Sci. 2018;53(1):29–39.
22. Serpooshan V, Zhao M, Metzler SA, Wei K, Shah PB, Wang A, et al. The effect of bioengineered acellular collagen patch on cardiac remodeling and ventricular function post myocardial infarction. Biomaterials. 2013;34(36):9048–55.
23. Gaetani R, Feyen DAM, Verhage V, Slaats R, Messina E, Christman KL, et al. Epicardial application of cardiac progenitor cells in a 3D-printed gelatin/hyaluronic acid patch preserves cardiac function after myocardial infarction. Biomaterials. 2015;61:339–48.
24. Jang J, Park HJ, Kim SW, Kim H, Park JY, Na SJ, et al. 3D printed complex tissue construct using stem cell-laden decellularized extracellular matrix bioinks for cardiac repair. Biomaterials. 2017;112:264–74.
25. Bejleri D, Streeter BW, Nachlas ALY, Brown ME, Gaetani R, Christman KL, et al. A bioprinted cardiac patch composed of cardiac-specific extracellular matrix and progenitor cells for heart repair. Adv Healthc Mater. 2018;7(23): e1800672.
26. Yeung E, Fukunishi T, Bai Y, Bedja D, Pitaktong I, Mattson G, et al. Cardiac regeneration using human-induced pluripotent stem cell-derived biomaterial-free 3D-bioprinted cardiac patch in vivo. J Tissue Eng Regen Med. 2019;13(11):2031–9.
27. Omoto ACM, Gava FN, Silva CAA, Silva HB, Parente JM, Costa RM, et al. Lack of scarring is not always a sign of cardiac health: functional and molecular characterization of the rat heart's following chronic reperfusion. PLoS ONE. 2018;13(12): e0209190.
28. Nicotra T, Desnos A, Halimi J, Antonot H, Reppel L, Belmas T, et al. Mesenchymal stem/stromal cell quality control: validation of mixed lymphocyte reaction assay using flow cytometry according to ICH Q2(R1). Stem Cell Res Ther. 2020;11(1):426.

Publisher's Note